

## A Biomimetic Approach to Asymmetric Acyl Transfer Catalysis

Elizabeth R. Jarvo, Gregory T. Copeland, Nikolaos Papaioannou, Peter J. Bonitatebus, Jr., and Scott J. Miller\*

*Contribution from the Department of Chemistry, Merkert Chemistry Center, Boston College, Chestnut Hill, Massachusetts 02467-3860**Received September 2, 1999*

**Abstract:** Small peptide catalysts containing modified histidine residues are reported that effect enantioselective acylation reactions. The catalysts described include octapeptide  $\beta$ -hairpins (e.g., **11**) that exhibit high selectivities (up to  $k_{\text{rel}} = 51$ ), tetrapeptide  $\beta$ -turns (e.g., **7**) that afford moderate selectivities (up to  $k_{\text{rel}} = 28$ ), and several simple derivatives of the modified histidine amino acid that do not exhibit appreciable enantioselectivity. Supporting structural studies ( $^1\text{H}$  NMR and X-ray) are presented which lead to the proposal of a model in which catalyst rigidity and structural complexity contribute to higher degrees of enantioselection. A covalently rigidified octapeptide (**20**) is prepared through solid-phase Ru-catalyzed ring-closing metathesis; kinetic evaluation of this peptide reveals that substituents along the peptide backbone may be more important than covalent stabilization of a structural motif. Detailed kinetics studies on the most selective peptide catalysts are presented that suggest the reactions are first order in catalyst and substrate. Additional kinetic studies indicate unambiguously that enantioselectivities are due to specific *acceleration* of reaction for one substrate enantiomer, rather than the *deceleration* of the reaction for the other. The results are presented in the context of a possible enantiomer-specific hydrogen-bonding interaction in the stereochemistry-determining step for these processes.

## Introduction

The enzymes that carry out enantio- and regioselective reactions are typically highly complex macromolecules. The complexity is, in part, due to the cell's need to engage enzymes in a variety of biochemical tasks. Stereoselective organic transformations represent a small subset of the functions that complete enzymes will execute.<sup>1</sup> What fraction of an enzyme's structure is necessary and what secondary structural motifs are optimal to carry out stereoselective reactions when a polypeptide is exempt from biological life-activities? To address these questions, we are studying synthetic peptides, composed exclusively of  $\alpha$ -amino acid monomers, that catalyze kinetic resolutions. Our studies indicate that these minimal  $\alpha$ -amino acid containing systems can catalyze acyl transfer reactions with  $k_{\text{rel}}$  values that reflect substantial enantiomer differentiation.

Enantioselective interactions of chiral substrates with enzymes are of central interest to molecular recognition and biological catalysis. At the heart of such selectivity is the ability of the enzyme to process one enantiomer of a given substrate while the other does not react. The basis for enzymatic enantiomer discrimination is frequently attributed to specific chiral interactions of the substrate with the enzyme.<sup>2</sup> Of note, however, is that while useful mnemonic devices have been derived to predict which substrates will give good selectivities, detailed mecha-

nistic understanding for the basis of these selectivities is often difficult to acquire.<sup>3,4</sup> Small-molecule mimics of enzymes offer practical advantages for catalyst development from the standpoints of (1) more straightforward analogue synthesis and (2) potentially easier mechanistic analysis.<sup>5</sup> Many important studies of stereoselective recognition of chiral peptidic hosts and guests have shed light on some of the factors that are the determinants of ground-state enantioselection.<sup>6</sup> In contrast, investigations of enantioselectivity with peptide-like enzyme mimics in a catalytic context have received substantially less attention.<sup>7</sup>

We recently reported a series of small peptides that are capable of effecting kinetic resolutions of functionalized secondary alcohols.<sup>8</sup> As shown in Scheme 1, these small-molecule catalysts are designed to include functional groups capable of carrying out nucleophilic catalysis of acyl transfer reactions of

(4) For an intriguing application of one such mnemonic, see: Griffith, D. A.; Danishefsky, S. J. *J. Am. Chem. Soc.* **1996**, *118*, 9526–9538.

(5) (a) Breslow, R. *Acc. Chem. Res.* **1995**, *28*, 146–153. (b) Murakami, Y.; Kikuchi, J.; Hiseada, Y.; Hayashida, O. *Chem. Rev.* **1996**, *96*, 721–758. (c) Kirby, A. J. *Angew. Chem., Int. Ed. Engl.* **1996**, *35*, 707–724.

(6) For representative examples, see: (a) Jeong, K.-S.; Muhldorf, A. V.; Rebek, J., Jr. *J. Am. Chem. Soc.* **1990**, *112*, 6144–6145. (b) Liu, R.; Sanderson, P. E. J.; Still, W. C. *J. Org. Chem.* **1990**, *55*, 5184–5186. (c) Cristofaro, M. F.; Chamberlin, A. R. *J. Am. Chem. Soc.* **1994**, *116*, 5089–5098. (d) Garcia-Tellado, F.; Albert, J.; Fan, E.; Hamilton, A. D. *J. Chem. Soc., Chem. Commun.* **1991**, 1761–1763. (e) Wilcox, C. S. *Chem. Soc. Rev.* **1993**, *22*, 383–395.

(7) For representative enantioselective catalysts that rely exclusively on peptide or a peptide-like functionality, see: (a) Sigman, M. S.; Jacobsen, E. N. *J. Am. Chem. Soc.* **1998**, *120*, 4901–4902. (b) Iyer, M. S.; Gigstad, K. M.; Namdev, N. D.; Lipton, M. J. *Am. Chem. Soc.* **1996**, *118*, 4910–4911. (c) Cleij, M. C.; Drenth, W.; Nolte, R. J. M. *J. Org. Chem.* **1991**, *56*, 3883–3891. (d) Tanaka, K.; Mori, A.; Inoue, S. *J. Org. Chem.* **1990**, *55*, 181–185. (e) Agami, C.; Puchot, C.; Sevestre, H. *Tetrahedron Lett.* **1986**, *27*, 1501–1504. (f) For a representative approach that involves a de novo designed protein, see: Broo, K. S.; Brive, L.; Ahlberg, P.; Baltzer, L. *J. Am. Chem. Soc.* **1997**, *119*, 11362–11372.

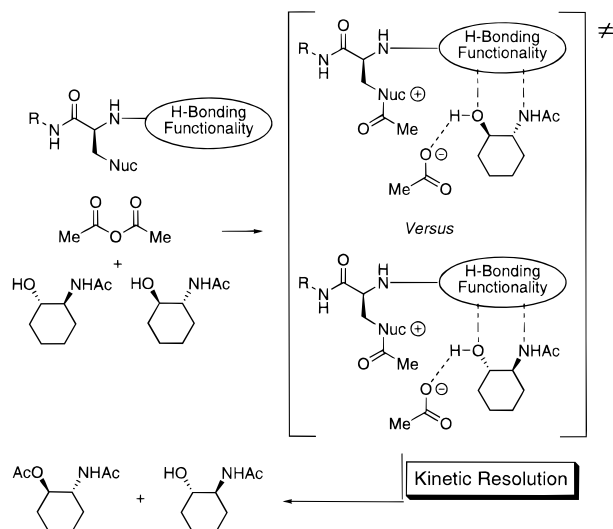
(8) (a) Miller, S. J.; Copeland, G. T.; Papaioannou, N.; Horstmann, T. E.; Ruel, E. M. *J. Am. Chem. Soc.* **1998**, *120*, 1629–1630. (b) Copeland, G. T.; Jarvo, E. R.; Miller, S. J. *J. Org. Chem.* **1998**, *63*, 6784–6785.

(1) For reviews, see: (a) Wong, C.-H.; Whitesides, G. M. *Enzymes in Synthetic Organic Chemistry*; Elsevier: Oxford, U.K., 1994. (b) Johnson, C. R. *Acc. Chem. Res.* **1998**, *31*, 333–341 and references therein.

(2) (a) Lamzin, V. S.; Dauter, Z.; Wilson, K. S. *Curr. Opin. Struct. Biol.* **1995**, *5*, 830–836. (b) Ingles, D. W.; Knowles, J. R. *Biochem. J.* **1967**, *104*, 369–377. (c) Fersht, A. *Enzyme Structure and Mechanism*; Freeman: San Francisco, CA, 1977. (d) Feng, S.; Schreiber, S. L. *J. Am. Chem. Soc.* **1997**, *119*, 10873–10874.

(3) For impressive examples, see: (a) Lee, T.; Sakowicz, R.; Martichonok, V.; Hogan, J. K.; Gold, M.; Jones, J. B. *Acta Chem. Scand.* **1996**, *50*, 697–706. (b) Derewenda, Z. S.; Wei, Y. *J. Am. Chem. Soc.* **1995**, *117*, 2104–2105.

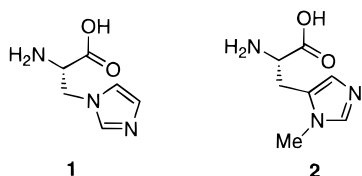
## Scheme 1



secondary alcohols and anhydrides. We projected that capture of the anhydride by the nucleophile would result in diastereomeric transition states of different energies on the basis of differential interactions of substrate enantiomers with the chiral environment created by the peptide. An initial objective of our study was to capitalize on differential hydrogen-bonding interactions between various substrates and catalysts.

## Results and Discussion

**Initial Catalyst Design.** Our initial design considerations focused on the two primary components of the catalyst structure: (i) the nature of the nucleophilic group and (ii) the structure of the hydrogen-bonding domain. After consideration of the known nucleophilic catalytic moieties (e.g., (dialkylamino)pyridines, phosphines, and *N*-alkylimidazoles),<sup>9,10</sup> we settled on the *N*-alkylimidazoles for our first-generation systems. The decision was based on both their ease of synthesis and the adequate catalytic efficiencies these moieties offer. To maximize enzymatic mimicry, we made the arbitrary choice to localize the nucleophilic moiety within an  $\alpha$ -amino acid side chain—a typical subunit within the well-known constructs of naturally occurring functional peptides. Accordingly, the two monomers, (*S*)- $\beta$ -*N*-imidazolylalanine (**1**)<sup>11</sup> and  $\pi$ (Me)-histidine (**2**)<sup>12</sup> emerged as reasonable nucleophilic amino acids.



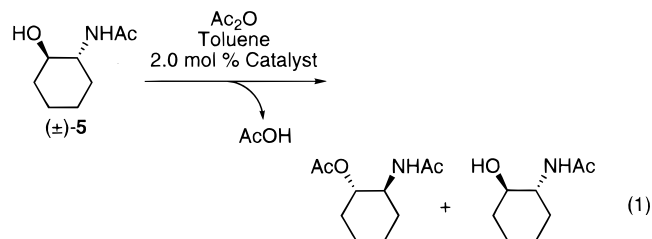
Our approach necessitated that acylated imidazolium ion intermediates be localized within the catalyst structure such that

(9) (a) Guibe-Jampel, E.; Bram, G.; Vilkas, M. *Bull. Soc. Chim. Fr.* **1973**, 1021–1027. (b) Höfle, G.; Steglich, W.; Vorbrüggen, H. *Angew. Chem., Int. Ed. Engl.* **1978**, *17*, 569–583. (c) For the *N*-alkylimidazoles, a general base-type mechanism cannot be excluded. See: Pandit, N. K.; Connors, K. A. *J. Pharm. Sci.* **1982**, *71*, 485–491.

(10) For representative, nonenzymatic enantioselective nucleophilic catalysts, see: (a) Vedejs, E.; Chen, X. *J. Am. Chem. Soc.* **1996**, *118*, 1809–1810. (b) Vedejs, E.; Daugulis, O. *J. Am. Chem. Soc.* **1999**, *121*, 5813–5814. (c) Tao, B.; Ruble, J. C.; Hoic, D. A.; Fu, G. C. *J. Am. Chem. Soc.* **1999**, *121*, 5091–5092. (d) Kawabata, T.; Nagato, M.; Takasu, K.; Fujii, K. *J. Am. Chem. Soc.* **1997**, *119*, 3169–3170. (e) Oriyama, T.; Imai, K.; Hosoya, T.; Sano, T. *Tetrahedron Lett.* **1998**, *39*, 397–400.

secondary H-bonding interactions between substrates and catalysts would be feasible during the acyl transfer step of the reaction mechanism. To maximize the opportunity for such transition-state organization, we incorporated **1** into the  $\beta$ -turn structure that was projected to result from the proline–aminoisobutyric acid (Pro-Aib) sequence.<sup>13,14</sup> Thus, compound **3** became our first-generation catalyst. A series of <sup>1</sup>H NMR experiments verified that **3** exists as a unique conformation in nonpolar solvents (e.g., CDCl<sub>3</sub>) and that it resembles the illustrated type II  $\beta$ -turn shown in Figure 1. For example, solvent titrations revealed that the chemical shift of the  $\alpha$ -methylbenzamide proton is relatively insensitive to increasing *d*<sub>6</sub>-DMSO concentration in C<sub>6</sub>D<sub>6</sub>/*d*<sub>6</sub>-DMSO mixtures (Figure 1a).<sup>15</sup> In contrast, the Aib(NH) and BOC(NH) protons shift dramatically downfield in response to increasing DMSO concentration. The temperature dependence of the chemical shifts, as well as infrared spectra in dilute solutions, are consistent with the assignment. The NOESY spectrum revealed a substantial cross-peak (circled in Figure 1b) between the Aib(NH) and the Pro(C $\alpha$ -H), supporting the type II assignment. Finally, control peptide **4**, where the imidazole is replaced with a phenyl ring, proved to be a crystalline solid from which an X-ray structure could be determined (Figure 1c).<sup>16</sup> Notable is the fact that the solution structure of **3** closely resembles the solid-state structure of **4** (relevant dihedral angles for **4**:  $\phi_{i+1} = -51^\circ$ ,  $\psi_{i+1} = +128^\circ$ ;  $\phi_{i+2} = +62^\circ$ ,  $\psi_{i+2} = +25^\circ$ ).

**Asymmetric Acylation with Tetrapeptide Catalysts.** Preliminary experiments demonstrated that H-bonding interactions between substrates and catalysts are kinetically relevant and that the imidazole moiety is crucial for catalysis.<sup>17</sup> The possible kinetic intervention of H-bonding interactions suggested that highly organized, stereodifferentiating transition states might be possible. Evaluation of test substrate **5** in a kinetic resolution revealed that this is indeed the case. Initial studies showed that ( $\pm$ )-**5** undergoes kinetic resolution in the presence of catalyst **3** (2 mol %, PhCH<sub>3</sub>, 0 °C) with a  $k_{rel}$  ( $k_{S,S}/k_{R,R}$ ) value of 12.6 (eq 1).<sup>18</sup> The same peptide catalyst was found to exhibit an enhanced



$k_{rel}$  value of 17 at higher dilution, and at 25 °C. Polar solvents such as CH<sub>3</sub>CN and protic media (*t*-BuOH as an additive) result

(11) (a) Arnold, L. D.; Kalantar, T. H.; Vederas, J. C. *J. Am. Chem. Soc.* **1985**, *107*, 7105–7109. (b) Tohodo, K.; Hamada, Y.; Shiori, T. *Synlett* **1994**, 247–248.

(12) Beyerman, H. C.; Maat, L.; Van Zon, A. *Recl. Trav. Chim. Pays-Bas* **1972**, *91*, 246–250.

(13) (a) Prasad, B. V. V.; Balam, H.; Balam, P. *Biopolymers* **1982**, *21*, 1261–1273. (b) Venkatachalapathi, Y. V.; Balam, P. *Biopolymers* **1981**, *20*, 1137–1145.

(14) (a) Ravi, A.; Balam, P. *Tetrahedron* **1984**, *40*, 2577–2583. (b) Rose, G. D.; Gierasch, L. M.; Smith, J. A. *Adv. Protein Chem.* **1985**, *37*, 1–109.

(15) For an interpretation of chemical shift dependences as a function of temperature in C<sub>6</sub>D<sub>6</sub> solvent, see: Venkatachalapathi, Y. V.; Balam, P. *Biopolymers* **1981**, *20*, 625–628.

(16) Crystallographic data may be found in the Supporting Information.

(17) Peptide **4** does not catalyze acyl transfer under the present conditions at an appreciable rate. This experiment rules out amide catalysis as the sole source of the reactivity and selectivity we observe: Titskii, G. D.; Litvinenko, L. M. *Zh. Obshch. Khim.* **1970**, *40*, 2680–2688.

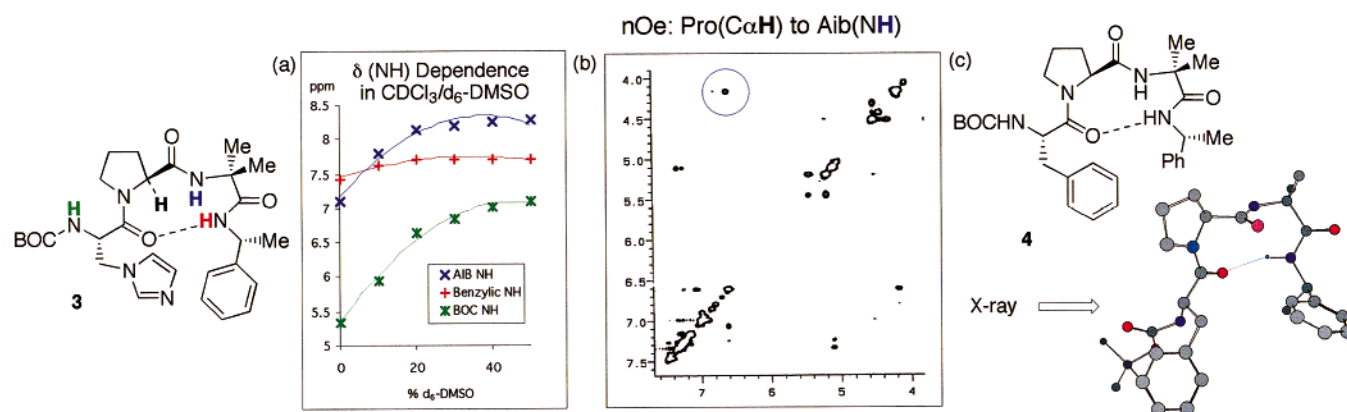
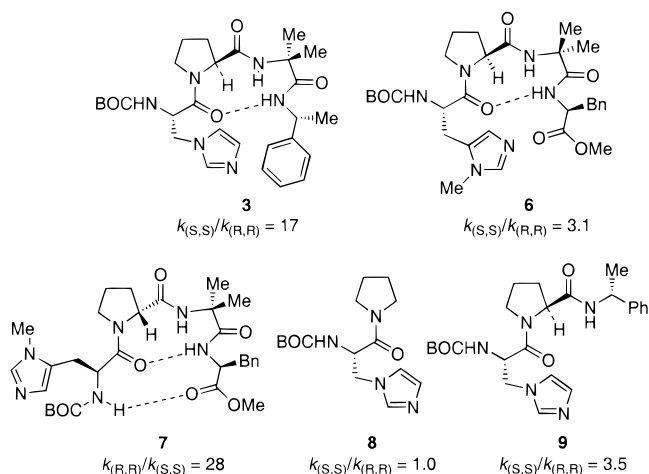


**Figure 1.** (a) Chemical shift dependences of amide NH protons of peptide **3** as a function of solvent composition. (b) NOESY spectrum of peptide **3** ( $CDCl_3$  solvent). (c) X-ray crystal structure of peptide **4** (hydrogen bond inferred).

in reactions that are far less enantioselective ( $k_{rel} \approx 1$ ). These observations are consistent with the postulate that H-bonding interactions are central to reaction selectivity. Further studies revealed a strong dependence of selectivity on catalyst conformation. In particular, *diastereomeric* peptides **6** and **7** give rise to acylation reactions with *opposite enantiospecificities*. Whereas peptide **6** (containing the L-Pro-Aib sequence) effects the catalytic resolution of ( $\pm$ )-**5** with a  $k_{rel}$  value of 3.1 (56% conversion), diastereomeric peptide **7** (containing the D-Pro-Aib sequence) is significantly more selective ( $k_{rel} = 28$ , 58% conversion), acylating the opposite enantiomer.<sup>19,20</sup> Furthermore, NMR experiments analogous to those applied to peptide **3** revealed that **6** exists predominantly as the illustrated  $\beta$ -turn; related experiments indicated that **7** possesses an additional intramolecular H-bond, consistent with the  $\beta$ -hairpin structure shown in Chart 1. Finally, pyrrolidine-substituted catalyst **8**, which is devoid of any secondary structure, does not promote acylation with any enantiodifferentiation. The truncated dipeptide **9**, incapable of adopting a  $\beta$ -turn structure, gives rise to a modest  $k_{rel}$  value of 3.5 under similar conditions.

**Octapeptides as Enantioselective Acylation Catalysts.** The increased selectivity exhibited by the D-Pro catalyst **7** suggested that enhanced rigidity achieved through increased structural complexity might lead to more selective catalysts. In this regard, we sought to extend the  $\beta$ -hairpin structure we had observed with peptide **7** to include several additional amino acids. Recent advances in the peptide design literature document the propensity of a D-Pro-Gly dipeptide to line up extended  $\beta$ -hairpin structures for certain peptide sequences.<sup>21</sup> Stimulated by this observation, we prepared octapeptide **11** containing the D-Pro-

**Chart 1**



Gly sequence. For comparison purposes, we prepared the analogous peptide **12** in which the D-Pro of **11** is replaced with L-Pro (Figure 2). Octapeptide **11** exhibits an extremely sharp  $^1H$  NMR spectrum (10 mM,  $CDCl_3$ ), consistent with the presence of a unique conformation in  $CDCl_3$ . Related peptides prepared by Balaram<sup>21d</sup> had been demonstrated to possess the four intramolecular hydrogen bonds shown for structure **11**. In fact, when octapeptide **11** is employed in the kinetic resolution of substrate ( $\pm$ )-**5**, excellent enantioselection is obtained ( $k_{rel} = 51$ ; 50% conversion). In contrast, the L-Pro-Gly octapeptide **12** exhibits an extremely broad  $^1H$  NMR spectrum (10 mM,  $CDCl_3$ ), reflecting either a degree of conformational mobility or peptide aggregation. Indeed, peptide **12** proves to be a far less selective catalyst, affording a substantially lower  $k_{rel} = 7$  (46% conversion) under analogous conditions.

**Kinetic Resolutions of Other Substrates.** With catalysts in hand that exhibited reasonably high selectivities for the six-membered-ring substrate **5**, we sought to examine the generality of these catalysts for other substrates (Table 1). The corresponding seven- and five-membered-ring 1,2-hydroxyamides **13** and **14** were examined, as was the cyclopentene-derived hydroxyamide **15**. Evaluation of the acylation reactions of the four substrates in the presence of the D-Pro octapeptide **11**, the D-Pro tetrapeptide **7**, and the L-Pro octapeptide catalyst **12** revealed the following facts. For each of the three catalysts the rigid six-membered-ring substrate **5** participates in the most selective reaction (entry 1, octapeptide **11**,  $k_{rel} = 51$ ; entry 5, tetrapeptide **7**,  $k_{rel} = 28$ ; entry 9, octapeptide **12**,  $k_{rel} = 7$ ). (2) For the cycloheptane derivative **13**, the D-Pro octapeptide **11**

(18) (a)  $k_{rel} = s$ -values ( $k_{rel} = k_{fast}/k_{slow}$ ) were calculated according to the method of Kagan. See: Kagan, H. B.; Fiaud, J. C. *Top. Stereochem.* **1988**, *18*, 249–330. (b) Reaction selectivities and conversions were determined in analogy to the method we reported previously.<sup>8</sup> See the Supporting Information for details. (c) The absolute sense of chirality of **5-Ac** and **5** was assigned according to the method of Jacobsen: Schaus, S. E.; Larrow, J. F.; Jacobsen, E. N. *J. Org. Chem.* **1997**, *62*, 4197–4199.

(19) For comparative examples of the conformational influence of L-Pro vs D-Pro residues in short peptides, see: (a) Haque, T. S.; Little, J. C.; Gellman, S. H. *J. Am. Chem. Soc.* **1996**, *118*, 6975–6985. (b) Karle, I. L.; Awasthi, S. K.; Balaram, P. *Proc. Natl. Acad. Sci. U.S.A.* **1996**, *93*, 8189–8193. (c) Raghothama, S. R.; Awasthi, S. K.; Balaram, P. *J. Chem. Soc., Perkin Trans. 2* **1998**, 137–143.

(20) Peptides were prepared according to standard solid-phase peptide synthesis protocols and purified by silica gel chromatography, or preparative HPLC. See the Supporting Information for details.

(21) (a) Stanger, H. E.; Gellman, S. H. *J. Am. Chem. Soc.* **1998**, *120*, 4236–4237. (b) Haque, T. S.; Gellman, S. H. *J. Am. Chem. Soc.* **1997**, *119*, 2103–2104. (c) Struthers, M. D.; Cheng, R. P.; Imperiali, B. *Science* **1996**, *271*, 342–345. (d) Raghothama, S. R.; Awasthi, S. K.; Balaram, P. *J. Chem. Soc., Perkin Trans. 2* **1998**, 137–143.

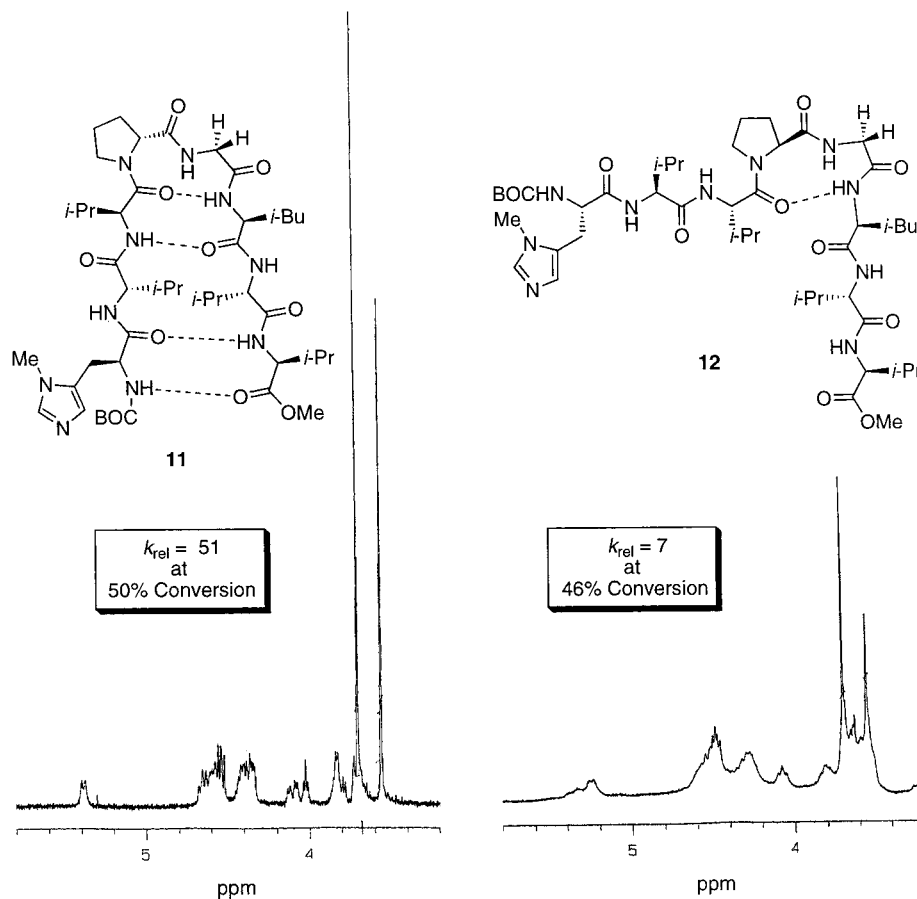


**Figure 2.** D-Pro-Gly octapeptide **11** and L-Pro-Gly octapeptide **12** and the corresponding  $\alpha$ -regions of the  $^1\text{H}$  NMR spectra ( $\text{CDCl}_3$ , 10 mM).

**Table 1.** Selectivities for Various Substrates in Kinetic Resolutions with Peptide Catalysts<sup>a</sup>

entry	catalyst	racemic substrate	conversion, %	$k_{\text{rel}}$
1	D-Pro octapeptide <b>11</b>	<b>5</b>	50	51
2		<b>13</b>	45	15
3		<b>14</b>	49	27
4		<b>15</b>	35	1
5	D-Pro tetrapeptide <b>7</b>	<b>5</b>	49	28
6		<b>13</b>	51	17
7		<b>14</b>	56	6
8		<b>15</b>	49	4
9	L-Pro octapeptide <b>12</b>	<b>5</b>	46	7
10		<b>13</b>	56	2
11		<b>14</b>	45	3
12		<b>15</b>	45	1

<sup>a</sup> Reactions were conducted with 1–2 mol % catalyst (5.9 mM in substrate,  $\text{PhCH}_3$  solvent) at 25 °C. Conversions and enantioselectivities were measured by chiral GLC (Chiraldex GTA). See the Supporting Information for details.

and the D-Pro tetrapeptide **7** effect kinetic resolution with nearly identical efficiencies, affording  $k_{\text{rel}}$  values of 15 and 17, respectively (entries 2 and 6, Table 1). In contrast, the L-Pro octapeptide **12** gives rise to a much less selective reaction ( $k_{\text{rel}} = 2$ ; entry 10). (3) Cyclopentane **14** proved a somewhat better substrate for catalyst **11**, with its kinetic resolution exhibiting  $k_{\text{rel}} = 27$  (entry 3). However, as shown in entries 7 and 11, both D-Pro tetrapeptide **7** and the L-Pro octapeptide **12** are much less selective catalysts for this substrate ( $k_{\text{rel}} = 6$  and 3,

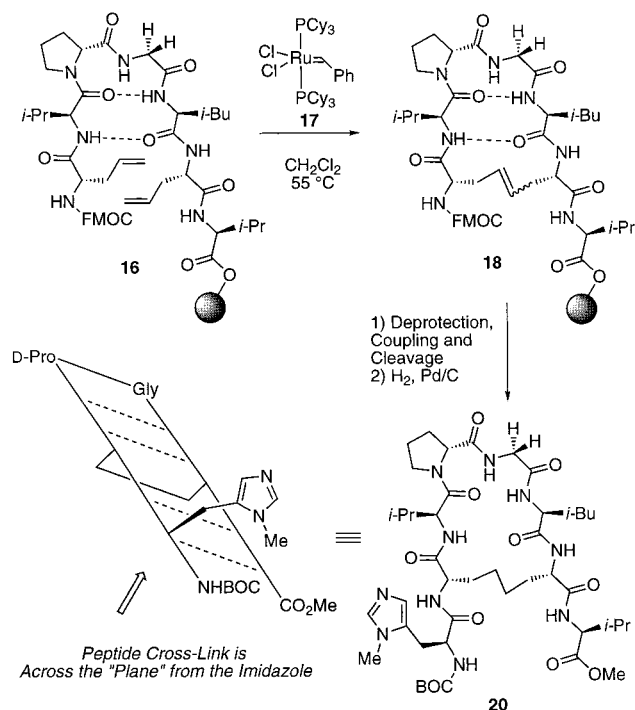
respectively). (4) With the octapeptide catalysts, the *cis*-1,3-acetamidocyclopentene derivative **15** was processed in an essentially nonselective reaction ( $k_{\text{rel}} \cong 1$ ; entries 4 and 12). However, the structurally more simple tetrapeptide catalyst **7** effects kinetic resolution of substrate **15** with modest but appreciable enantioselection ( $k_{\text{rel}} = 4$ , entry 8). While the above data do not readily lend themselves to a working model to explain reaction enantioselectivity, they do indicate that structurally defined octapeptide  $\beta$ -hairpins provide a motif upon which highly enantioselective catalysts may be based. It also appears that the conformational rigidity afforded by the  $\beta$ -hairpin itself is one determinant of the enantiodifferentiation afforded by a given octapeptide catalyst (**11** vs **12**).

The high selectivity observed with the octapeptide  $\beta$ -hairpin stimulated further study of this structural motif. In particular, we set out to examine the impact of covalent rigidification on the efficiency of the kinetic resolutions. For hairpin strand cross-linking we employed Ru-catalyzed ring-closing olefin metathesis (RCM), previously demonstrated to be effective in peptides.<sup>22</sup> In particular, we chose to cross-link the residues in the ( $i + 1$ ) and ( $i + 6$ ) positions (Scheme 2). Our choice was based on a structural model of the  $\beta$ -hairpin that indicates the localization of these residues on the sheet face opposite the  $\pi(\text{Me})$ -histidine imidazole moiety. Thus, solid-support-bound diene **16** (HMBA-AM-polystyrene) was treated with Ru-benzylidene catalyst

(22) (a) Schwab, P.; Grubbs, R. H.; Ziller, J. W. *J. Am. Chem. Soc.* **1996**, *118*, 100–110. (b) Miller, S. J.; Blackwell, H. E.; Grubbs, R. H. *J. Am. Chem. Soc.* **1996**, *118*, 9606–9614.

(23) Following the catalytic RCM reaction, the resin was treated with tris(hydroxymethyl)phosphine to facilitate removal of the Ru-containing entities: Maynard, H. D.; Grubbs, R. H. *Tetrahedron Lett.* **1999**, *40*, 4137–4140. We thank Heather D. Maynard for providing a sample of the phosphine.

## Scheme 2



**17** to afford cyclic peptide **18**.<sup>23</sup> Cleavage of a sample of the peptide from the resin at this stage revealed that the RCM reaction had proceeded in essentially quantitative yield (no acyclic peptide could be detected by electrospray mass spectrometry or 400 MHz <sup>1</sup>H NMR spectroscopy). Peptide **18** was then elaborated on the solid support to complete the octapeptide synthesis. Cleavage from the resin under mild, nonpimerizing conditions (Et<sub>3</sub>N/MeOH/DMF, 64 h), followed by catalytic hydrogenation, afforded cyclic peptide **20** as a single compound. The peptide was then purified using standard HPLC techniques. Acyclic peptide **19** was also synthesized to provide an appropriate acyclic control peptide.

Examination of rigidified peptide **20** and its acyclic analogue **19** revealed these peptides to be less enantioselective than the original octapeptide **11** in selected kinetic resolutions. For example, as shown in entries 1 and 5 of Table 2, peptides **19** and **20** effect the kinetic resolution of substrate **5** with  $k_{rel}$  values of 20 and 12, respectively (cf.  $k_{rel}$  = 51 with **11**). Similarly, for the seven- and five-membered-ring substrates **13** and **14**, reduced  $k_{rel}$  values are observed relative to the original D-Pro octapeptide **11**. For the seven-membered-ring species **13** (entries 2 and 6), peptides **19** and **20** give rise to kinetic resolutions with  $k_{rel}$  values of 8 and 4, respectively (cf.  $k_{rel}$  = 17 with **7**); for the five-membered-ring compound **14** (entries 3 and 7), acyclic octapeptide **19** and cyclic octapeptide **20** effect kinetic resolutions with  $k_{rel}$  values of 12 and 8, respectively (cf.  $k_{rel}$  = 27 with **11**). For the cyclopentene derivative **15** (entries 4 and 8), only nonselective catalysis was observed.

It is noteworthy that for each of the three 1,2-acetamidocycloalkanol (**5**, **13**, and **14**) the *acyclic* peptide **19** is a more selective catalyst than the *covalently rigidified* analogue **20**. This observation may be in accord with certain models of enzyme action that suggest a modicum of flexibility is necessary to chaperone a substrate throughout a given reaction coordinate.<sup>24</sup> It is also noteworthy that the exchange of the isopropyl group side chains in the (*i* + 1) and (*i* + 6) positions of octapeptide

**Table 2.** Selectivities for Various Substrates in Kinetic Resolutions With Acyclic Peptide Catalyst **19** and Cyclic Analog **20**<sup>a</sup>

entry	catalyst	racemic substrate	conversion, %	$k_{rel}$
1	acyclic octapeptide <b>19</b>	<b>5</b>	51	20
2		<b>13</b>	52	8
3		<b>14</b>	51	12
4		<b>15</b>	35	1
5	cyclic octapeptide <b>20</b>	<b>5</b>	48	12
6		<b>13</b>	56	4
7		<b>14</b>	50	8
8		<b>15</b>	31	1

<sup>a</sup> Reactions were conducted with 1–2 mol % catalyst (5.9 mM in substrate, PhCH<sub>3</sub> solvent) at 25 °C. Conversions and enantioselectivities were measured by chiral GLC (Chiraldex GTA). See the Supporting Information for details.

**11** for allyl groups in peptide **19** (Val → allylGly) has such a dramatic effect on the enantioselectivity exhibited by these catalysts. This is particularly intriguing in light of the fact that this substitution is on the  $\beta$ -hairpin face *opposite* the reactive imidazole moiety. While a detailed explanation for this phenomenon is difficult to formulate at the present time, it is nonetheless clear that remote substituent effects on the octapeptide catalyst can have a large impact on the enantioselectivity exhibited by peptides in this class.

**Kinetic Studies.** Having discovered peptides that provided high  $k_{rel}$  values, we sought to understand the basis for their selectivities. As reported previously, circumstantial evidence points to the involvement of H-bond contacts between catalyst and substrate that are retained in the enantioselectivity-determining step of the catalytic cycle. However, it was not clear at the outset of our studies whether a unique catalyst and substrate molecule might interact in the transition state (as opposed to aggregates), as implied in Scheme 1. It was therefore of interest to determine the order of the reaction in substrate and catalyst.

Kinetic runs were performed under our optimized conditions of high dilution (PhCH<sub>3</sub>, 25 °C), and disappearance of starting material was monitored by capillary GC (Figure 3). Plots of ln([**5**]<sub>init</sub>/[**5**]) versus time were found to be linear for both the fast- and the slow-reacting enantiomers. In addition, the plots of log(initial rate) versus log[**5**]<sub>init</sub> were found to be linear with slopes of approximately 1 (fast enantiomer, slope 1.09,  $R^2$  = 0.995; slow enantiomer, slope 1.16,  $R^2$  = 0.994).<sup>25,26</sup> Similarly, kinetic evaluation of the effect of catalyst concentration afforded plots of log(initial rate) versus log[**11**]<sub>init</sub> that were also linear with slopes near unity (fast enantiomer, slope 0.93,  $R^2$  = 0.987; slow enantiomer, slope 1.23,  $R^2$  = 0.996). These results are most consistent with a reaction mechanism wherein the order of substrate and catalyst is each 1, under conditions of high dilution and in the initial rate range.

(25) Birk, J. P. *J. Chem. Educ.* **1976**, *53*, 704–707.

(26) Kinetic experiments were also carried out on the single enantiomers. Pseudo-first-order kinetics were observed in these experiments as well.

(24) (a) Koshland, D. E., Jr. *Proc. Natl. Acad. Sci. U.S.A.* **1958**, *44*, 98–104. (b) Breslow, R. *Supramol. Chem.* **1995**, *6*, 41–47.

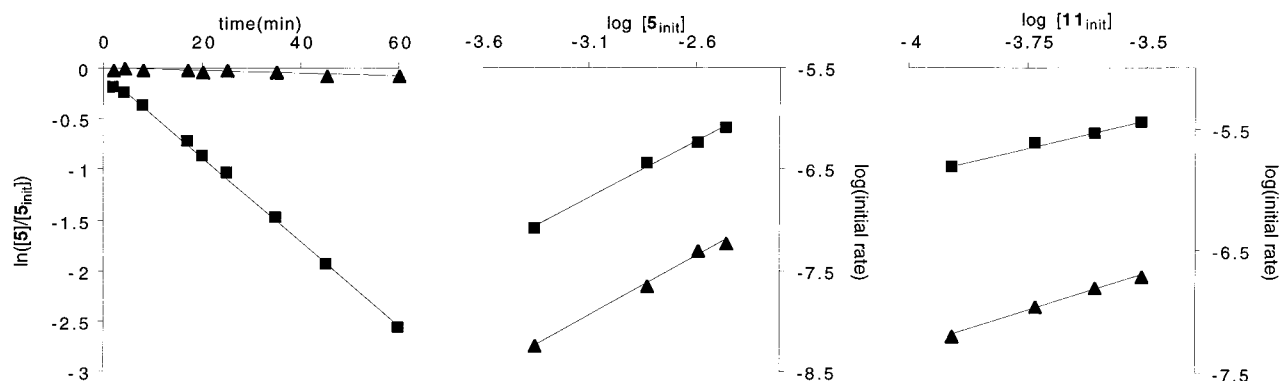


**Figure 3.** Kinetic plots for kinetic resolutions of substrate **5** employing peptide **11** as catalyst. Squares represent (*R,R*)-**5** (fast enantiomer), and triangles represent (*S,S*)-**5** (slow enantiomer). All reactions were conducted in PhCH<sub>3</sub> at 25 °C. See Supporting Information for details.

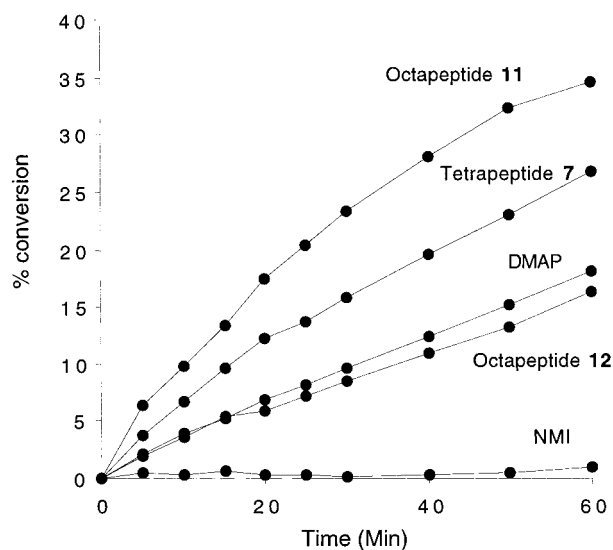


**Figure 4.** Relative rates of acylation of substrate **5** with various catalysts. All reactions were carried out with 2.5 mol % catalyst (5.9 mM in substrate) in PhCH<sub>3</sub> at 25 °C.

At this point, we wished to determine whether the basis of the enantioselectivity is due to an accelerative process (e.g., an enantiomer-specific transition-state H-bonding interaction) or a decelerative interaction (an enantiomer-specific steric effect). Therefore, we compared the rates of the acylation of ( $\pm$ )-**5** catalyzed by different peptides (tetrapeptide **7**, octapeptide **11**, and octapeptide **12**) to those observed with the well-known acylation catalysts *N*-methylimidazole (NMI) and (dimethylamino)pyridine (DMAP). Reactions were conducted under identical conditions and at the optimized level of dilution. Under these conditions, *each of the peptides is substantially more active than NMI* (Figure 4). Interestingly, the most selective catalyst in the series, octapeptide **11**, is also the most active. Similarly, D-Pro tetrapeptide **7** is more active than L-Pro octapeptide **12**. The relative *activity* of these two catalysts is also mirrored by their relative *selectivity*: that is, tetrapeptide **7** exhibits a higher  $k_{rel}$  value than octapeptide **12** ( $k_{rel}(\mathbf{7}) = 28$ ;  $k_{rel}(\mathbf{12}) = 7$ ). Perhaps most surprising is that peptides **7** and **11** proved more active

(27) Under more concentrated conditions (200 mM in substrate), DMAP is more active than tetrapeptide **7**. Since absolute selectivities are also lower with peptide catalysts at higher concentrations, we tentatively attribute this phenomenon to peptide-catalyst deactivation through aggregation. See the Supporting Information for details.

(28) (a) Shimizu, K. D.; Snapper, M. L.; Hoveyda, A. H. *Chem. Eur. J.* **1998**, *4*, 1885–1889. (b) Francis, M. B.; Jamison, T. F.; Jacobsen, E. N. *Curr. Opin. Chem. Biol.* **1998**, *2*, 422–428.

(29) Copeland, G. T.; Miller, S. J. *J. Am. Chem. Soc.* **1999**, *121*, 4306–4307.

than the superacylation catalyst DMAP under the conditions of optimized dilution.<sup>27</sup> These relative rate experiments are consistent with the proposal that the selectivities obtained with peptides are due to accelerative effects rather than decelerative ones. In combination with the  $k_{rel}$  values, it appears that the observed enantioselectivities are due to the specific rate acceleration of one enantiomer's reaction pathway, rather than the specific deceleration of the other's.

### Conclusions

The combination of the observed enantioselectivities, first-order kinetics for substrate and catalyst, and relative rate data for the peptide-based alkylimidazoles relative to NMI implicate a specific transition-state geometry between peptide and substrate. Preliminary attempts to observe associations between catalysts and substrates directly with NMR techniques have so far proven unsuccessful. In this context, it may be that the ground-state binding energies are too weak to allow definitive characterization. Nevertheless, the studies presented above demonstrate that peptidic nucleophilic catalysts represent viable candidates for the development of additional enantioselective catalysts. While the goal of achieving substrate general catalysts remains elusive, it is apparent that small peptides contain sufficient information to differentiate enantiomers of certain substrates in kinetic resolutions. The modularity of peptide structures, the ease of incorporating functional groups into amino acid monomers, and the possibility of parallel and combinatorial syntheses of corresponding libraries bode well for future developments in this field.<sup>28</sup> Current efforts in our laboratory are focused on this and related objectives.<sup>29</sup>

### Experimental Section

Full experimental details for all experimental aspects of the study, including compound characterization, are available in the Supporting Information.

**Acknowledgment.** We are grateful to the National Science Foundation for generous support in the form of a CAREER Award (Grant No. CHE-9874963). In addition we thank the National Institutes of Health (Grant No. GM-57595) and Research Corp. (Grant No. RIA-116) for generous research support. Acknowledgment is also made to the donors of the Petroleum Research Fund, administered by the American Chemical Society, for partial support. S.J.M. is a Cottrell Scholar of Research Corp.

**Supporting Information Available:** Text and tables giving full experimental details for all aspects of the study, including compound characterization, and tables giving X-ray crystallographic data for peptide **4**. This material is available free of charge via the Internet at <http://pubs.acs.org>.